Ab initio study of the surface of a decagonal Al-Co-Ni quasicrystal

M. Krajčí,[1,2] J. Hafner,[1] and M. Mihalkovič[2]
[1]*Institut für Materialphysik and Center for Computational Materials Science, Universität Wien, Sensengasse 8/12, A-1090 Wien, Austria*
[2]*Institute of Physics, Slovak Academy of Sciences, Dúbravská cesta 9, SK-84228 Bratislava, Slovak Republic*
(Received 16 November 2005; published 14 April 2006)

The structure, stability, and electronic properties of the tenfold surface of the decagonal Al-Co-Ni quasicrystal have been investigated using *ab initio* density-functional methods. The structural model of the surface has been derived from the recently resolved structure of the *W*-(AlCoNi) approximant phase. The bulk quasicrystal can be cleaved at the flat *A* plane or at the puckered *B* plane. We investigate the stability and electronic properties of the surface for both possible terminations. The simulated scanning-tunneling microscopy (STM) images of the *A* and *B* surfaces show that despite their significantly different atomic structure and chemical composition both surfaces exhibit quite similar STM images. The electronic structure of the approximant phase is characterized by a pseudogap at the Fermi level. The pseudogap at the surface is partially covered and the positions of *d* bands of both transition metals undergo a substantial shift towards lower binding energies.

DOI: 10.1103/PhysRevB.73.134203 PACS number(s): 61.44.Br, 68.35.Bs, 71.20.−b, 71.23.Ft

I. INTRODUCTION

Quasicrystals are of great interest due to their potential for creating unusual structural forms of matter having extraordinary physical properties. Quasicrystalline surfaces are also important for possible technological applications. For example, surfaces of quasicrystals exhibit high hardness and good tribological properties such as low surface friction; they also show high oxidation resistance. During the last decade significant progress has been made in the preparation and characterization of surfaces of icosahedral and decagonal quasicrystals. Great attention has been focused on the properties of the surfaces of stable quasicrystals such as icosahedral (*i*) Al-Pd-Mn and decagonal (*d*) Al-Co-Ni, which were studied by various experimental methods.[1–4]

The improved efficiency of computational methods and the increasing performance of the available computers allows one to obtain interesting physical information also from *ab initio* calculations on realistic structural models. In a previous paper[5] we have studied the structure, stability, and electronic properties of the fivefold surface of icosahedral Al-Pd-Mn quasicrystals. In the present work we apply our *ab initio* methods to the investigation of the tenfold surface of a *d*-Al-Co-Ni quasicrystal.

A prerequisite for an *ab initio* calculation of the properties of a quasicrystal is a good structural model. In comparison with icosahedral quasicrystals the structure of decagonal quasicrystals with only two-dimensional quasiperiodicity seems to be more easily accessible to intuitive interpretations. Despite this fact, so far no satisfactory, generally accepted model of decagonal Al-Co-Ni quasicrystals exists. The modeling of the structure of decagonal Al-Co-Ni quasicrystals has a long history.[6–16] On the basis of experimental information from diffraction studies, a number of structural models for *d*-Al-Co-Ni alloys have been proposed. The large number of distinct stable decagonal phases in the *d*-Al-Co-Ni system makes it difficult to model the quasiperiodic structure on a systematic basis. Thermodynamic and structural studies[18–21] revealed the existence of a very complex phase diagram of the pseudobinary AlCo-AlNi system in the stability range of the decagonal phases, showing a large structural variety. Ritsch *et al.*[21] report eight different structural modifications of decagonal phases. Most stable decagonal phases exist only at high temperatures in the range of 700–1100 K. The largest region of quasicrystalline stability exists at compositions close to $Al_{70}Ni_{15}Co_{15}$. However, the complexity of the phase diagram is not the main reason for the persisting difficulties in the structural modeling of decagonal Al-Co-Ni quasicrystals. It appears that the main obstacle arises from the existence of a certain degree of disorder in the decagonal phases.[17] The electron diffraction patterns observed for Co-rich decagonal phases exhibit features characterized by pentagonal or rhombic tilings forming columnar clusters with a decagonal section of 20 Å in diameter. Models with a perfectly deterministic arrangement of atoms, based on large, highly symmetric decagonal clusters, appear to disagree with the available structural data.

A significant breakthrough in structural modeling has been promoted by the recent discovery of the *W* approximant in the Al-Co-Ni system. The atomic structure of this phase has been resolved by Sugiyama *et al.*[16] using x-ray diffraction. The structure of the *W*-(AlCoNi) phase is closely related to that of the decagonal Al-Co-Ni quasicrystal. It provides fundamental information on the atomic arrangement for the columnar clusters commonly observed in Al-Co-Ni decagonal quasicrystals. A preliminary five-dimensional (5D) hyperspace model of the quasicrystal structure derived from the *W* approximant has been proposed by Deloudi *et al.*[22] As at present the *W*-(AlCoNi) phase is the only approximant to the decagonal quasicrystal with experimentally determined atomic positions, it is natural to base our model of the bulk *d*-Al-Co-Ni quasicrystal on the *W*-(AlCoNi) phase.

The characterization of tenfold decagonal surfaces should be in principle simpler than that of the surfaces of icosahedral quasicrystals because their structure is periodic in the direction perpendicular to the surface, and therefore only a few terminations are possible. Scanning tunneling micros-

copy (STM) is one of the most frequently used experimental probes for the analysis of the local structure of quasicrystalline surfaces. However, as STM images reflect actually only the electronic charge density at a certain distance above the surface and energies slightly above or below the Fermi level (depending on the position of the tip, the tunneling voltage and the direction of the current), but not its atomic structure, independent complementary information from theoretical models linking the atomic positions and the electron density is very desirable. In this paper we report our results of a structural modeling of the *d*-Al-Co-Ni surface. Investigation of surface relaxation and reconstruction, calculations of the charge density distribution at the surface, and simulated STM images of the surface are presented.

II. COMPUTATIONAL METHOD

The charge density distribution and other electronic properties have been calculated using advanced local-density-functional techniques. We have used the Vienna *ab initio* simulation package VASP (Refs. 23 and 24) to perform *ab initio* electronic structure calculations and structural optimizations. The theoretical background of VASP is density-functional theory within the local density approximation. The wave functions are expanded in plane waves. The Hamiltonian is based on pseudopotentials derived in framework of the projector-augmented-wave (PAW) method.[24] VASP performs an iterative diagonalization of the Kohn-Sham Hamiltonian. The plane-wave basis allows us to straightforwardly calculate Hellmann-Feynman forces acting on the atoms. The total energy may by optimized with respect to the positions of the atoms within the cell. The calculations were performed within the the generalized-gradient approximation (GGA)[25] to the exchange-correlation functional. VASP has also been used to calculate charge distributions. The projector-augmented-wave version[24] of VASP calculates all-electron eigenstates and not only pseudoeigenstates; hence, it produces very realistic electron densities.

The possibility to calculate the interatomic forces allows us to investigate possible surface relaxations or reconstructions. We are able to study the change of the positions of atoms at and near the surface relative to the bulk termination in response to the broken bonds at the surface.

III. STRUCTURAL MODEL OF SURFACE OF *d*-Al-Co-Ni

A structural model of a decagonal surface is obtained from the model of the bulk decagonal quasicrystal by cleaving at a proper quasiperiodic plane perpendicular to the periodic axis.

A. Structural model of *d*-Al-Co-Ni

Because of the high computational effort, *ab initio* methods require structural models consisting of at most several hundreds of atoms. So far in our *ab initio* studies of quasicrystals we successfully used quasicrystalline approximants as models representing the infinite quasicrystal. At present the *W* phase is the only reasonably large approximant with experimentally determined positions of atoms. The choice of the *W*-(AlCoNi) approximant phase as a model of the bulk *d*-Al-Co-Ni quasicrystal is therefore quite natural. The electron probe microanalysis[16] gives the composition of the *W*-(AlCoNi) phase as $Al_{71.8}Co_{21.1}Ni_{7.1}$. This composition is close to the Co-rich decagonal phases. As x-ray diffraction does not provide the information necessary for distinguishing the two transition-metal (TM) atoms, Ni and Co, the structural model of Sugiyama *et al.*[16] for the *W* phase is in fact a model for an Al-M approximant with the composition $Al_{71.8}M_{28.2}$. The structural model is represented by the list of atomic positions. The chemical identity of TM sites cannot be determined on the basis of the structural data alone. Moreover, in the refinement of Sugiyama *et al.*[16] some atomic sites have fractional Al-M occupancy. For *ab initio* studies it is mandatory to have a model with an unambiguously defined chemical identity of the atomic sites and without fractional occupancies.

The computational power of present computers makes it possible to perform a refinement of the chemical order of the model via total energy minimizations. Mihalkovič and Widom have performed an extensive *ab initio* study of the ternary Al-Ni-Co phase diagram.[26] The structure of the *W* approximant was refined by optimizing the total energy, under the constraint of a fixed overall content of the three species Al, Ni, and Co. They successfully resolved the chemical identity of the transition-metal sites and determined the occupancies of the mixed Al-M sites as well. In the case of binary systems the thermodynamic stability of a phase is determined by the position of the total energy of the phase with respect to a tie-line connecting points corresponding to other stable phases. In the case of ternary phases an analogous construction to the tie-line is a tie-plane. The structural model of the *W* phase obtained by Mihalkovič and Widom is only 13 meV/atom above the tie-plane defined by the stable phases Al_3Co in the *oI*96 structure (Pearson notation), Al_5Co_2 (*hP*28), and Al_3Ni_2 (*hP*5). This is an extraordinarily good result as for models of quasicrystalline approximants values of 40–80 meV/atom are common. The explicit examples can be found in the alloy database of Ref. 26. The composition of their model of the *W* phase is $Al_{71.70}Co_{20.75}Ni_{7.55}$—i.e., very close to that experimentally determined by electron probe microanalysis.[16] In addition to this model they proposed several other chemical variants. We have decided to use the variant with the composition $Al_{70.78}Co_{14.61}Ni_{14.61}$. The composition of this approximant is closer to the composition $Al_{71.8}Ni_{14.8}Co_{13.4}$ of the decagonal quasicrystal used for the surface studies reported, e.g., in Ref. 27.

The space group of the *W* phase is Cm (No. 8) with lattice parameters $a=39.668$ Å, $b=23.392$ Å, and $c=8.158$ Å. As the monoclinic angle β is equal to 90.05° the elementary cell has approximately an orthorhombic shape. The *W* phase belongs to the decagonal approximant phases with 8 Å periodicity along the decagonal axis. We note that the translation period of other decagonal modifications can be equal to 4 Å. The structure of the *W* phase can be described in terms of alternating flat (*A*) and puckered (*B*) atomic layers perpendicular to the *c* axis. The structure of the flat *A* layer at $z=0$ corresponds to that at $z=0.5$ (A') which is shifted by a half period along the *a* axis. The puckered layers at $z=0.25$

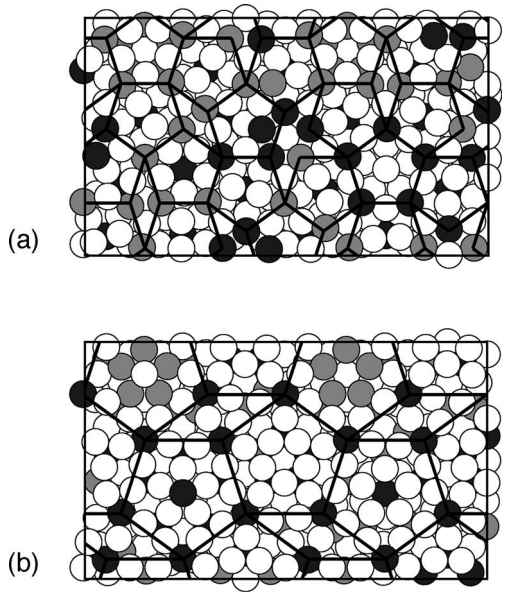

FIG. 1. A view of the atomic structure of *A* (a) and *B* (b) surfaces. The positions of atoms are displayed by circles: Al, open circles; Co, dark gray circles; Ni, light gray circles. To represent the quasiperiodic ordering the surfaces are covered by planar tilings of pentagons, thin rhombi, and boat. The tiling represents a network of the transition-metal (TM) atoms in the surface plane. Because of the different content of TM atoms, the tilings are different in both planes. The *A* plane is more TM rich. The edge length of the tiling superposed on the *A* plane is 4.68 Å. The edge of tiles in the *B* plane is 7.58 Å.

and $z=0.75$ are related to each other by mirror planes at $z=0$ and $z=0.5$. The structure of the *W* approximant can be thus described as a $ABA'B$ stacking of atomic planes along the *c* axis. The orthorhombic elementary cell consists of 534 atoms. The coordinates of atoms can be found in the alloy database accessible online; see Ref. 26. For bulk calculations it is possible to choose a monoclinic primitive cell with half the number of atoms.

B. Cleavage planes forming tenfold surfaces

A structural model of a quasicrystalline surface of *d*-Al-Co-Ni is obtained from a model of the decagonal Al-Co-Ni quasicrystal by cleaving it at a proper plane. The structural model of the *W* approximant naturally offers two possible termination planes. The bulk quasicrystal can be cleaved at the flat *A* plane or at the puckered *B* plane. In the present work we shall consider both possible terminations.

The quasiperiodic ordering of atoms at the surface can be visualized by covering the surface by a planar tiling. However, the choice of the tiling is not completely unambiguous. One can put on the surface various kinds of tilings. So far no generally accepted tiling has been proposed. As the primary aim of our present work is to discuss the details of the local atomic structure and the chemistry of bonding at the surface we decided to choose a tiling that suitably represents a network of the transition-metal atoms in the surface plane.

Figure 1 shows atomic structure of the two surfaces. In the TM-rich *A* layer [Fig. 1(a)], the lines connect TM atoms separated by 4.68 Å in the plane, forming a network of edge-sharing pentagons. Pentagon centers are even or odd vertices of a hexagon-boat supertiling, suggesting a way to generalize the *W* phase structure to higher-order approximants to the quasicrystal. One can distinguish two kinds of pentagons. The decoration of say the "even"pentagons is fivefold symmetric (in some of the pentagons the chemical decoration breaks this symmetry), while for "odd" pentagons the interior motif breaks the fivefold symmetry. In the bulk the orientation of pairs of Al atoms near the centers of the "odd" pentagons is the result of a special ordering phenomenon with 8 Å periodicity described in terms of "channels" in which the structure accommodates 3 Al atoms per 8 Å period.[28] Because of a different content of TM atoms, the tilings are different in both planes. The *A* plane is more TM rich. The edge of the tiling superposed on the *A* plane is 4.68 Å. In the TM-poor *B* layer [see Fig. 1(b)] the size of tiles connecting TM atoms is 7.58 Å—i.e., $\tau=1.618\ldots$ times larger than that in the *A* plane. However, the tiling on the *A* surface cannot be simply considered as a τ-inflated tiling on the *B* surface. The relation of both tilings is presented in Fig. 2(a).

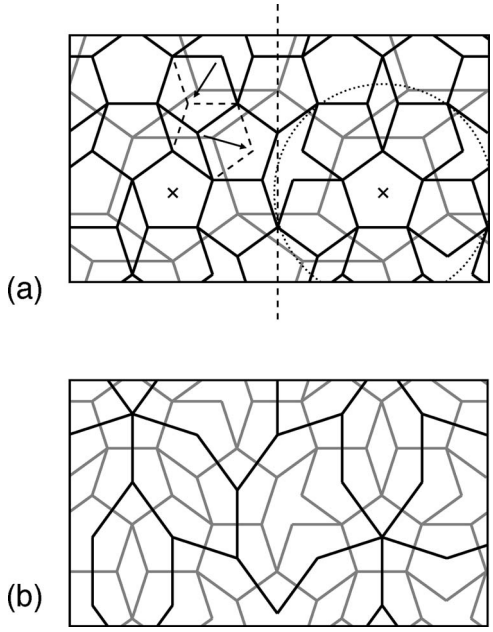

FIG. 2. The tilings representing the quasiperiodic ordering in the *W* approximant. Part (a) compares the *A* (black lines) and *B* (gray lines) tilings; cf. the previous figure. The vertical dashed line represents the plane dividing the *W* approximant into two parts. While the *B* tiling is symmetric with repect to this plane, the *A* tiling is not symmetric. A few phason flips indicated by arrows can make the *A* tiling also symmetric. The left and right parts of the *A* tiling can be thus understood as two phason versions of the same structure. Small crosses mark the position of the centers of the 20-Å columnar clusters; the right one is indicated by a dotted circle. Part (b) shows the relation of the *A* tiling to a larger hexagon-boat (HB) tiling. A more general hexagon-boat-star (HBS) tiling is a possible candidate to represent the quasiperiodic order in the decagonal quasicrystal.

The vertical dashed line represents the plane dividing the *W* approximant into two parts. While the *B* tiling has trans-

lation symmetry—the right part of the tiling can be obtained by translating the left part by $a/2$—the A tiling does not possess such symmetry. Nevertheless, by introducing a few phason flips (and two more vertices) also the A tiling can acquire the same translation symmetry. After such a rearrangement one would get, e.g., a pentagonal star instead of the boat tile in the center. However, the vertices of such a symmetric tiling would not represent the network of TM atoms at the A surface anymore. If the phason flip is accompanied by an interchanging of an Al and a TM atom, the correct TM decoration of the vertices would be recovered. The left and right parts of the A tiling can be understood as two phason variants of the same structure.

The relation of the tilings to the 20-Å columnar clusters is indicated in Fig. 2(a). The positions of the 20-Å clusters are marked by small crosses. The columnar clusters are concentric with the pentagonal tiles of both A and B tilings. In the right part of Figs. 1 and 2(a) one can see the pentagonal symmetry and the atomic structure of two layers of the 20-Å cluster that Deloudi *et al.* propose as a candidate for modeling all kinds of superstructures in decagonal Al-Co-Ni.[22] In the left part of Fig. 2(a) one can actually see the geometrical structure of another two layers of this columnar cluster. The superposed A tiling shows that in the W phase the perfect pentagonal symmetry of the columnar cluster is partially broken in the A' plane.

The tiling consists of pentagons, thin rhombuses, and boat-shaped tiles. In other approximants one could expect also a pentagonal star. Each center of the pentagonal tiles in the A tiling can be considered as a vertex of a larger tiling. This larger tiling is in fact a part of the hexagon-boat-star (HBS) tiling; see Fig. 2(b). The HBS tiling is thus a possible candidate to represent the quasiperiodic order in larger approximants or in an infinite decagonal quasicrystal.

The atoms at the surface have bulk-relaxed positions. The effect of the surface relaxation on the position of atoms and a possible surface reconstruction will be discussed in Sec. III C. The centers of the TM coincide remarkably well with the vertices of the tiling. The internal decoration of the pentagons in the B plane maintains the pentagonal symmetry. Particularly interesting is the decoration of the interior of the pentagons by pairs of Al atoms. Such a configuration in a decagonal quasicrystal is surprising. The decoration of some other pentagonal tiles is irregular. It is a manifestation of the fine structure present in d-Al-Co-Ni quasicrystals.

C. Relaxation of atomic positions and surface reconstruction

The surfaces of solids can adopt a structure different from that of atomic layers in the bulk.[29] The existence of unsaturated bonds at the surface can lead to a rearrangement of positions of the atoms at the surface with a periodicity larger than that of the bulk-terminated surface. Such surface reconstructions are well known for covalently bonded solids with low-coordinated atomic sites at the surface. In metals, surface reconstruction is observed mainly on the more open surfaces. Since both surface terminations of the W approximant expose close-packed layers, no significant reconstructions are to be expected.

One has to distinguish between relaxation of atomic positions relative to their idealized positions in the bulk resulting from long-range forces and surface reconstruction which is a response to broken bonds at the surface. In a model with relaxed coordinates the position of each atom is shifted relative to its equilibrium position in response to the forces acting from the neighboring atoms. The relaxation can lead to significant displacements of atoms if models with idealized coordinates of atoms are relaxed. Relaxation leads to a modulation of the structure, but usually does not lead to a change of the topology of the structure. The spatial modulation of the ideal quasiperiodic structures resulting from long-range interatomic forces has been discussed in detail in our earlier works on higher-order approximants of i-Al-Zn-Mg and i-Al-Cu-Li.[30,31]

Our methods allow us to approach the problem of surface reconstruction superposed onto the relaxation. The positions of atoms in our model of the W approximant were already relaxed in the bulk structure. The relaxed coordinates of the atoms can be found in the alloy database of Ref. 26. In comparison with the experimentally determined positions of atoms[16] there are only a few insignificant differences, induced mostly by assigning a unique chemical identity to each atomic site in the relaxed model (in principle, a model represents just one of many different possible chemical decorations of the unit cell of the W phase). Otherwise a typical displacement of the relaxed coordinates in comparison with experimental ones was less than ≈ 0.1 Å.

For the surface relaxation one has to prepare a slab model of sufficient thickness. The number of atomic layers should be large enough to stabilize the bulk structure in the deeper layers. Generally, in the case of quasicrystalline surfaces it is not possible to take as many atomic layers as usual in the studies of surfaces of crystalline solids. The period of the W approximant perpendicular to the quasiperiodic plane is 8 Å. This corresponds to five atomic layers. In the case of the termination A one gets an $ABA'BA$ sequence of layers, for the B termination the $BABA'B$ sequence. Unfortunately, five atomic layers in the W approximant already lead to a structural model with more than 660 atoms in the computational cell. This is too big for an *ab initio* relaxation where the electronic structure must be recalculated after each move of the atoms. We have to restrict our relaxation studies to a smaller model. We have found that it is quite simple to divide the W approximant into two almost identical parts. Figure 1(b) shows that the periodicity of the B layers along the x axis is $a/2$. The A and A' planes are also identical when shifted by $a/2$ along the x axis. When skipping one atom in the A layer and one atom in A' it is possible to enforce periodicity with a half period along the x axis. One thus gets a structural model of an approximant with a half number of atoms than in the W approximant. Figure 2 shows the position of the plane where we cut the model into two parts. We call this smaller approximant the U approximant. The number of atoms in the elementary cell of the U approximant is 265. Such an approximant could in principle also exist in the phase diagram; however, it is clear that nature prefers the W approximant as it can accommodate 534 atoms—i.e., 4 more atoms than in two elementary cells of the U approximant.

We relaxed the positions of atoms in the U approximant. As we started the relaxation from already bulk-relaxed posi-

tions it is not surprising that the changes of atomic positions are quite minimal. It is known also from other studies[5,32] that in aluminum–transition-metal quasicrystals the transition-metal atoms have low mobility. We found that the changes of positions of Al atoms upon relaxation are also very small, below 0.15 Å.

Ferralis *et al.*[3] analyzed the structural relaxation of the quasicrystalline *d*-Al-Ni-Co surface using low-energy electron diffraction (LEED). They found differences in the interlayer spacing of near-surface layers compared with the spacing of atomic layers in the bulk. The outermost layer spacing is contracted by 10% relative to the bulk interlayer spacing, while the next layer spacing is expanded by 5%. We relaxed the surface by minimizing the forces acting on the atoms in two outermost layers of both sides of the slab, while the atoms in the central layer were fixed at their bulk positions. Contrary to the conclusions from the LEED analysis, the interlayer spacing between the two top most layer is essentially unchanged in our model. In our study d_{12}, defined as a distance between the centers of gravity of the positions of the atoms in the surface *B* layer and the next *A* layer, increased from its original value of 2.027 Å by 0.016 Å. Similarly small were changes of the next layer spacing between the next two layers. The interlayer spacing remained essentially unchanged regardless of whether the relaxed model had the *A* plane or the *B* plane at the surface. We admit that one possible explanation of this discrepancy with the experimental observation of Ferralis *et al.*[3] could be the limited thickness of our model.

IV. ELECTRONIC STRUCTURE OF *d*-Al-Co-Ni

The electronic structure represented by the density of electronic states is a sensitive probe reflecting the local structure and the chemical short-range order in solids.

A. Electronic structure of the bulk

Figure 3 presents the calculated total and partial densities of states (DOS) of the *W* approximant. The calculation has been performed for a monoclinic primitive cell containing 267 atoms. Because of the elongated shape of the primitive cell, three **k** points in the irreducible part of the Brillouin zone proved to be sufficient. The most remarkable feature of the calculated DOS is the existence of a deep minimum or a pseudogap at the Fermi level. The composition $Al_{189}Co_{39}Ni_{39}$ gives a position of the Fermi level just at the center of the deep minimum in the DOS. The coincidence of the position of the Fermi level and the deep minimum in the DOS is commonly interpreted as an electronic stabilization in terms of the Hume-Rothery mechanism.[35,36] In the case of nearly-free-electron *sp*-bonded quasicrystals like *i*-Al-Cu-Li,[31] *i*-Al-Zn-Mg,[33,34] and Zn-Mg-Y,[37] there are no doubts that this mechanism plays an essential role in the stabilization of these alloys. However, in the case of Al-M quasicrystals to which most of the decagonal quasicrystals, including *d*-Al-Co-Ni, belong, the situation is not so clear.[38] In the light of previous results the observation of a deep pseudogap in the DOS at the Fermi level is thus quite remarkable. Our calculations show that the deep pseudogap exists also in the DOS of the model of the *W* phase with the experimentally determined composition $Al_{71.8}Co_{21.2}Ni_{7.1}$; see Sec. III. The pseudogap is here even somewhat deeper; however, the Fermi level falls a little (0.09 eV) below the minimum. This result could indicate that the pseudogap is rather insensitive to the relative compositions of Co and Ni.

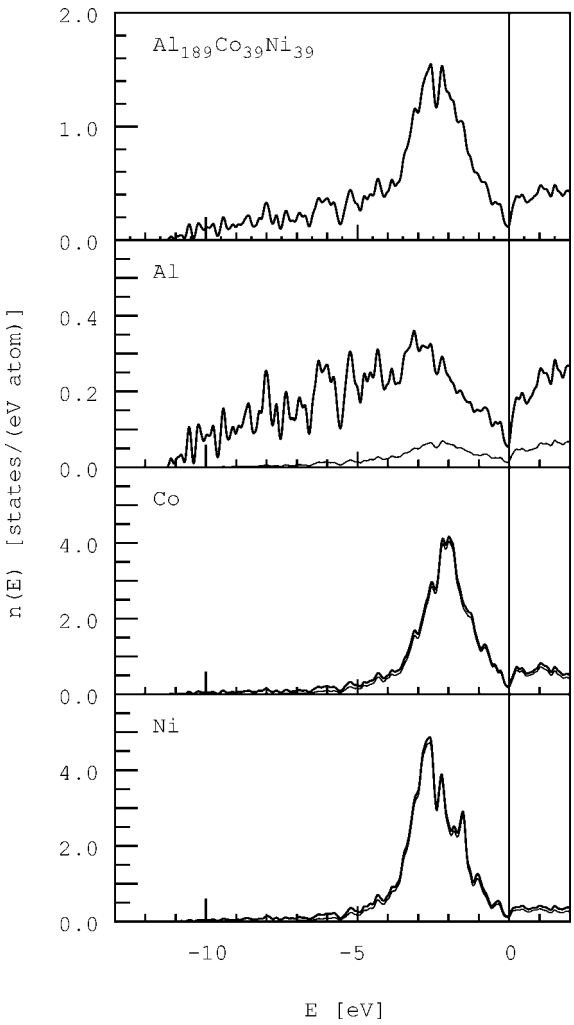

FIG. 3. The total and partial densities of states (DOS) of the *W* approximant representing bulk *d*-Al-Co-Ni quasicrystal. The most remarkable feature of the calculated DOS is the existence of a deep minimum or a pseudogap. The composition $Al_{70.78}Co_{14.61}Ni_{14.61}$ gives the position of the Fermi level just to the deep minimum in the DOS. The thin lines show a contribution of the *d* states to the DOS.

In our previous paper[11] on the electronic structure of the d-$Al_{0.70}Co_{0.15}Ni_{0.15}$ quasicrystal we performed an extensive study of the influence of the Al-M and Ni-Co ordering on the resulting DOS. Our model of *d*-Al-Co-Ni was based on the decoration of a Penrose tiling with a large rhombus edge by clusters with a diameter 20 Å. The internal structure of the 20-Å clusters was proposed by Hiraga, Sun, and Yamamoto;[8] the chemical ordering on these clusters (which cannot be determined by diffraction studies alone) was optimized so as to achieve an optimal agreement of the calculated electronic structure with the experimental spectra. We compared the

results of the electronic structure calculations with experimental photoemission[39–41] (PES) and soft-x-ray spectra.[42] An interesting outcome was that the DOS peaks corresponding to the Ni and Co *d* bands had almost the same position. In some of the chemical variants the peak in the Co *d* band was pushed down to even higher binding energies than the peak in the Ni *d* band. This is contrary to the positions expected from the relative *d*-band filling, but the reversal of the band positions has also been observed in soft-x-ray spectroscopy.[42] In the electronic structure of the *W* approximant representing the *d*-Al-Co-Ni quasicrystal one also observes that both *d* peaks are located close to each other. The symmetric Co DOS is peaked around its center of gravity at −2.1 eV. Although the asymmetric Ni DOS is peaked at somewhat lower energies around −2.8 eV its shoulder at −1.7 eV shifts the center of gravity of the Ni DOS to −2.3 eV—i.e., very close to that of the Co DOS.

B. Electronic structure at the surface

The DOS at the surface has been calculated on the *U* models with 8 Å thickness. Figure 4 shows the total and partial DOS at both surfaces. The pseudogap at the Fermi level is almost completely covered at the surface, especially at the *A* surface. Both Co and Ni *d* peaks are shifted by ≈0.5 eV to lower binding energies. Remarkably, at the *A* surface the Ni *d* band is still located at higher binding energies than the Co *d* band, while on the *B* surface the asymmetry of the Ni *d* band is reversed compared to the bulk with an absolute maximum closer to E_F than that of the Co *d* band. The partial DOS of both TM atoms is steeply ascending below the Fermi level while it is almost constant above the Fermi level. The different height of the main peak in the total DOS of both surfaces reflects the different content of TM atoms in the surfaces.

C. Comparison with the photoemission spectra

Figure 5 presents a comparison of the photoemission spectrum of the *d*-$Al_{0.70}Co_{0.15}Ni_{0.15}$ quasicrystal measured by Stadnik *et al.*[40,41] with simulated spectra of the *W* approximant with composition $Al_{70.78}Co_{14.61}Ni_{14.61}$ and with that of a crystalline Al_9CoNi phase. The ultraviolet photoelectron spectrum (UPS) was measured at low temperature and He II photons with an energy of 40.8 eV. The theoretical curves were calculated by weighting the partial densities of states with the photoionization cross sections of the elements and broadening by a convolution with the Gaussian resolution function with the resolution parameter of 0.5 eV. The theoretical curves are normalized to the common maximal height. The figure shows that in comparison with the experimental PES the position of the *d* bands in the *W* approximant is shifted by ≈0.8 eV to higher binding energies. The shift to higher binding energies is even larger for crystalline Al_9CoNi. The figure also shows the theoretical PES curves calculated from the DOS at the surface. The curves for both surfaces *A* and *B* are almost identical. As the *d* peaks of TM atoms in the surface DOS are shifted to lower binding energies, the main peak of simulated PES is now almost coincident with the experimental one. However, this coincidence cannot be simply interpreted as a good agreement with the experimental data. The contributions to the photoelectron intensity come not only from the uppermost surface but also from the atomic layers deeper in the bulk. In a more sophisticated approach one should compare with the experimental data a weighted average of bulk and surface DOS. A large difference between the simulated and experimental PES is observed also in the vicinity of the Fermi energy: a pronounced Fermi edge appears in the experimental spectrum and also in that calculated for the quasicrystalline surface, whereas for the bulk quasicrystalline and crystalline phases the existence of a deep pseudogap is evident. It is clear that the experimental data correspond to substantially higher DOS at the Fermi level than we observe for the *W* approximant. However, from a detailed analysis of the shape of the PES intensity in the vicinity of the Fermi edge Stadnik *et al.*[40,41] concluded, using a sophisticated fitting procedure, that the observed high DOS is still only 85% of "normal" DOS and hence the experimental data indicate the existence of a shallow Hume-Rothery pseudogap.

Very recently Suzuki *et al.*[43] investigated the electronic structure of the surface of the decagonal $Al_{72}Co_{16}Ni_{12}$ quasicrystal using metastable $He^*(2\,^3S, 1s2s)$ deexcitation spectroscopy (MDS). They clearly observed a pseudogap in the density of states at the topmost surface. They present also UPS (He I) data on the crystalline and quasicrystalline surfaces of Al-Co-Ni. The UPS spectrum shows a remarkable decrease of the states at E_F indicating the existence of a pseudogap in the electronic spectrum. The pseudogap was found to be shallower at the surface than in the bulk. Both these results are in agreement with our calculations. The findings of Suzuki *et al.*[43] concerning the depth of the pseudogap in the electronic spectrum of decagonal Al-Co-Ni are partially in conflict with the older data of Stadnik *et al.*[40,41] However, it is necessary to note that the data of Suzuki *et al.*[43] were obtained on the Co-rich decagonal quasi-crystal $Al_{72}Co_{16}Ni_{12}$ while in the work of Stadnik *et al.*[40,41] the composition of the decagonal phase was specified as $Al_{70}Co_{15}Ni_{15}$. This means that the composition of the quasicrystal examined by Suzuki *et al.* is closer to that of the *W* approximant (for which we find a pseudogap), while the composition of the specimen used by Stadnik *et al.* is very close to that of the Yamamoto model (for which theory does not predict a pseudogap). We have to conclude that the electronic structure of *d*-Al-Co-Ni should be reexamined with particular attention to both the composition and quasicrystalline structure of the sample and to the dependence of the spectra on the energy of the exciting photons and hence the escape depth of the photoelectrons.

V. ATOMIC STRUCTURE, CHARGE DENSITY DISTRIBUTION, AND STM IMAGE OF THE SURFACE

A. Atomic structure and the charge density distribution

Interesting information about the atomic structure of the surface can be derived from the electronic charge density distribution. Figure 6 displays the valence charge density distribution at both surfaces (black spots in both figures). The

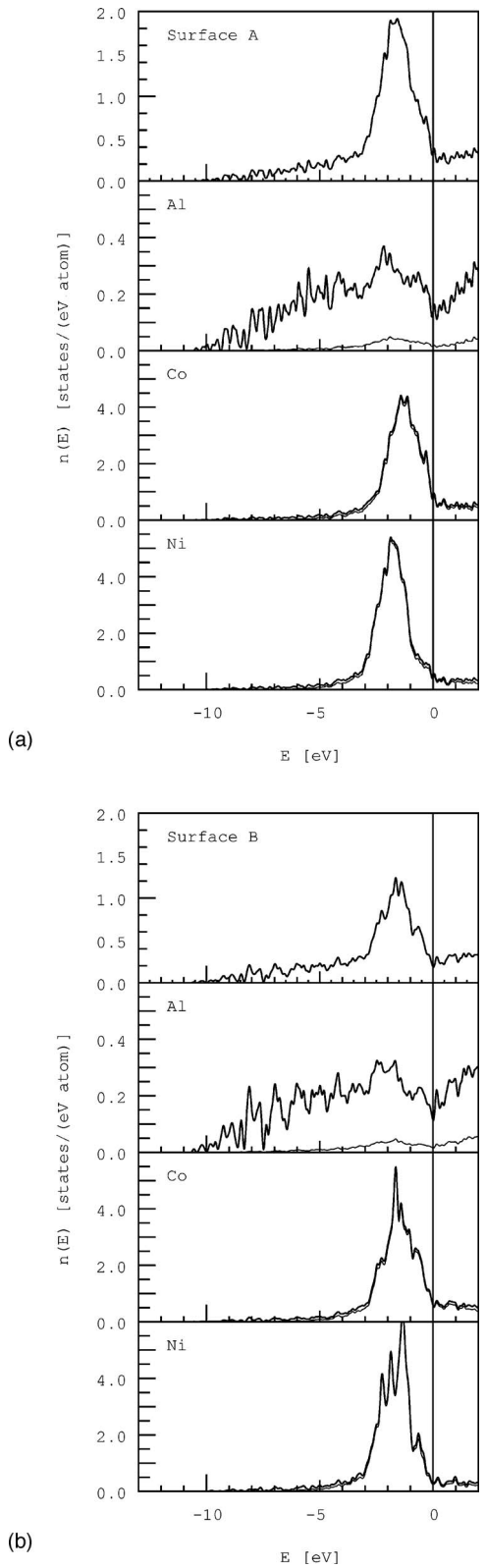

FIG. 4. Surface electronic DOS of the *A* (a) and *B* (b) surfaces. The total and partial densities of states at both surfaces are significantly different from those of bulk; cf. Fig. 3. The pseudogap is partially covered. In comparison with the position of the Co and Ni *d* bands in bulk the *d* bands in the surface DOS are shifted towards the Fermi level. Note a significant enhancement of the Al partial DOS at E_F.

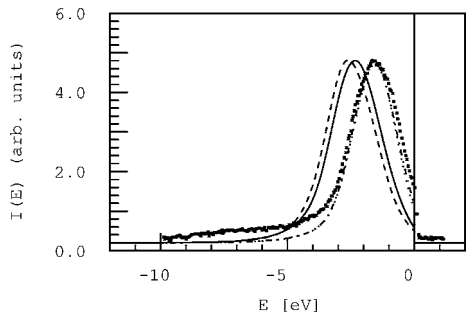

FIG. 5. Comparison of the measured photoemission spectrum (PES) of a *d*-$Al_{0.70}Co_{0.15}Ni_{0.15}$ quasicrystal (squares, data from Ref. 40), with simulated spectra of the *W* approximant with the $Al_{70.78}Co_{14.61}Ni_{14.61}$ composition. The solid line corresponds to the PES spectrum calculated from bulk DOS; the dashed curve shows for comparison the PES calculated for a crystalline Al_9CoNi phase (composition $Al_{64}Co_{18}Ni_{18}$) with the crystal structure of Al_9Co_2. The chain and dotted line correspond to the spectrum calculated from the surface DOS of *A* and *B* surfaces, respectively. The curves of the surface DOS for both surfaces are almost identical. The theoretical curves are normalized to the common maximal height.

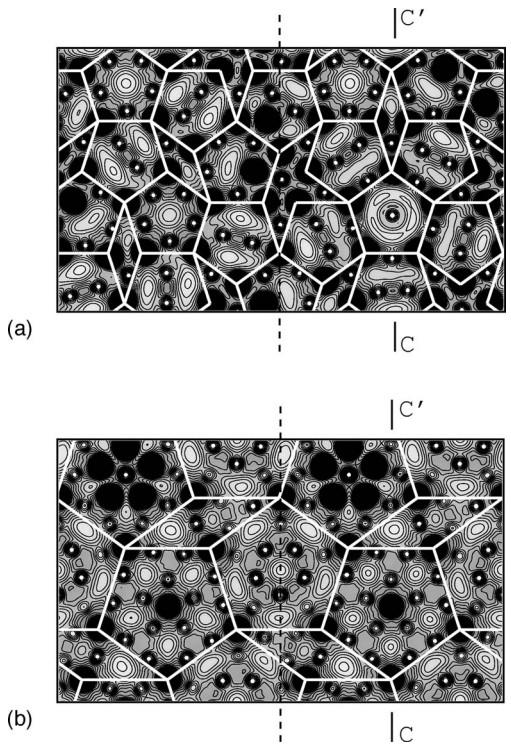

FIG. 6. The valence charge density distribution at the surfaces *A* (a) and *B* (b). The contour plots represent cuts through the charge density distribution at the position of the top layer (see also Fig. 7). The transition-metal atoms in the plane create a high local charge density (black circles). The positions of the Al atoms can be recognized as small circular islands of local density minima. The charge density distributions in the planes perpendicular to the surface intersecting along lines marked as CC' are presented in Fig. 7. The dashed lines represent the plane dividing the *W* approximant into two parts; cf. text.

position of the TM atoms is characterized by high valence charge densities. At the position of the Al atoms one observes small local valence charge density minima. Because of the different content of TM atoms in both termination planes, it is not surprising that the overall view of both surfaces is quite different. A closer inspection of the charge density shows a significant variation of the charge density between atoms at both surfaces. It is remarkable that in terms of the variation of the local electron density the roughness of the flat *A* surface is comparable to that of the puckered *B* surface. Particularly deep are the charge density minima in the pentagonal tiles of the *A* surface. Inside the pentagons formed by five TM atoms one observes from one to five additional atoms. The charge density minima are the most pronounced if inside the pentagons only one or two atoms are located, but a clear charge density minimum is formed even in the case where five atoms fill the pentagon.

At the *B* surface the internal decoration of the TM pentagons is regular. One can here also observe various charge density minima between the atoms. The surface charge density minima are important as attractive sites for possible adsorbate atoms. The results of our study of the formation of an adsorbate adlayer on the surface *d*-Al-Co-Ni quasicrystal will be published in a forthcoming paper.

Compared with the fivefold surface of *i*-Al-Pd-Mn there is one significant difference. In the case of the *d*-Al-Co-Ni surface there are no strong charge depletions corresponding to surface vacancies as we observed and reported in our recent work.[5] A direct comparison of the experimental images obtained from the scanning tunneling microscopy with the *ab initio*–calculated STM images revealed that the characteristic features of the images—the dark pentagonal holes (dark stars)—correspond just to the surface vacancies.[44]

The view on the surface valence charge density provides also information about interatomic bonding. As in any complex Al-M alloy one can expect also in the *W* approximant a high degree of covalency of bonding between Al and TM atoms.[45–48] An interesting bonding configuration between Al atoms only is observed at the *A* surface. At the midpoint between the pairs of Al atoms inside the pentagonal tiles one can recognize an enhanced charge density. This indicates a significant degree of covalency in the bonding between two Al atoms, as is also suggested by the deep pseudogap in the partial DOS. As such a bonding has been observed also in the charge density distribution of the bulk *W* approximant, one cannot identify these bonds as in-plane bonds that are formed due to a surface reconstruction. This suggests that this bonding configuration contributes to the stabilization of the decagonal quasicrystalline structure—as previously reported for crystalline TM-aluminides.[45–48]

Figure 7 represents a contour plot of the valence charge density distribution in the plane perpendicular to the quasiperiodic plane. The bonding with enhanced covalency can be observed also between the atomic planes. By the enhanced covalency of bonding we mean the enhanced bonding charge between the atoms, enhanced with respect to a homogeneous charge density distribution that would correspond to a purely metallic bonding. The bonding between the atomic planes is promoted by the Al-M interaction. The figure provides an impression of the surface corrugation. In comparison with

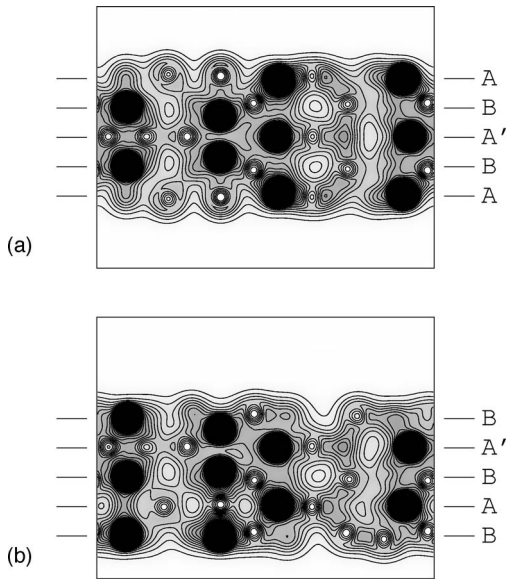

FIG. 7. Sections perpendicular to the surface displaying the profile of valence charge density distribution in the relaxed models of both surfaces *A* (a) and *B* (b). The contour plots represent cuts of charge density distribution at the position of lines *CC′* in Fig. 6. The relaxation has only minimal influence on the position of atoms. The figure shows the roughness of both surfaces.

the surface of *i*-Al-Pd-Mn here there are no such special structural defects as the surface vacancies observed at the fivefold surface of *i*-Al-Pd-Mn.[5,44] Otherwise the roughness of both *d*-Al-Co-Ni surfaces is comparable with that of the fivefold *i*-Al-Pd-Mn surface.

Although the valence charge density distribution provides important information about the structure of the surface and its chemistry, a link to comparable experimental information is still missing. STM imaging is considered as the most direct experimental tool for obtaining information about the structure of a surface. As the STM image is formed only by a part of the valence charge density distribution corresponding to a narrow energy interval around the Fermi level, the structure of the surface seen in the STM images can significantly differ from that presented by the valence charge distribution.

B. Simulated STM images of the surface

Simulated STM images of the surfaces have been calculated according to the Tersoff-Hammann approximation.[49] The contrast in the STM images reflects the local DOS determined by the tip position and the average over energy intervals around the Fermi level. The width of the energy interval is determined by the voltage between the tip and surface. Depending on the direction of the tunneling current STM can image occupied or unoccupied electron states. In the usual experimental setup the tip of the device is grounded. If the voltage of the sample to the tip is negative, the electrons flow from the occupied states of the sample to the tip. A positive polarity corresponds to imaging the unoccupied states.

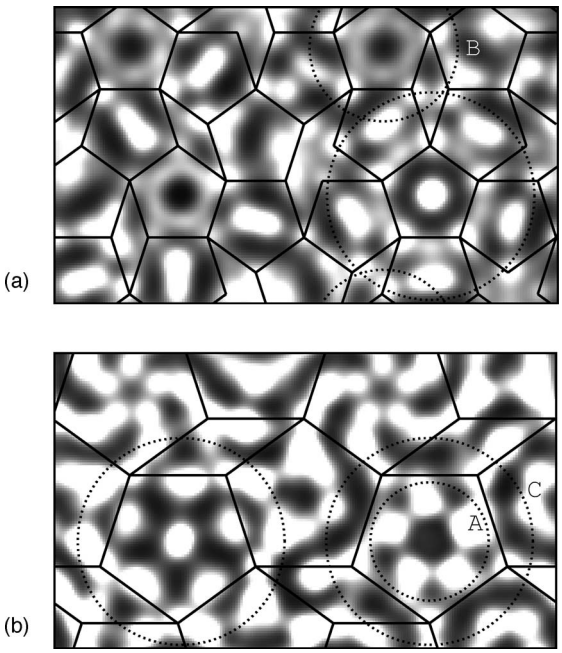

FIG. 8. STM images of the surfaces of the *W* approximant to *d*-Al-Co-Ni calculated from the surface charge density distribution. The calculation simulated a STM image measured at a voltage −1.0 V with the tip at constant height 2.0 Å above the surface plane. This size and polarity of the voltage correspond to contributions from occupied states up to −1.0 eV below the Fermi level. Parts (a) and (b) correspond to the *A* and *B* surfaces, respectively. The individual atoms are clearly recognized as bright spots. The dotted circles mark some pentagonal configurations; cf. Fig. 9 and text.

Figure 8 shows the calculated STM images of both surfaces for a tip-sample voltage of −1.0 eV. This corresponds to the imaging of the electronic density formed by the occupied states down to 1.0 eV below the Fermi level. In the narrow energy interval around the Fermi level the DOS (see Fig. 3) is quite symmetric. From this one would expect that for unoccupied states (positive voltage) the images are similar. However, the information on the electronic structure of the bulk presented in Fig. 3 can be misleading. The density of electronic states at the surface can be different from that of the bulk (see Fig. 4). In the vicinity of the Fermi level the partial DOS of Co and Ni atoms is not symmetric and therefore there will be a clear difference in the contribution of the TM atoms to the STM current from occupied and unoccupied states. From the comparison of the STM images measured for both tip polarities one could thus distinguish between Al and TM atoms. In a STM image taken at positive polarity (imaging unoccupied states) the brightness of spots corresponding to the TM atoms will substantially decrease.

Quasicrystals as complex metallic alloys exhibit a rather rich, spiky structure of the DOS. It is important to measure the STM current at rather large voltage such as to integrate over a larger part of the DOS around the Fermi level to obtain representative images of the surface. In the usual experimental setup STM measurements are performed more frequently for a constant tunneling current than for a constant height above the surface. Both types of measurements provide essentially the same information about the chemistry of the surface. In our calculations we prefer to present STM images for constant height. We found that STM images calculated for a constant height rather close to the surface are less diffuse than those calculated for constant current. The information about individual atoms can be thus clearly recognized without any additional Fourier filtering usually applied on the experimental images to improve their contrast. The STM images presented in Fig. 8 are calculated for a constant height of ≈2 Å above the surface. To simulate the contrast of the experimental STM image as presented in Fig. 9 the contrast of Fig. 8 has been further increased by the gamma correction ($I_{\text{out}}=I_{\text{in}}^{1/\gamma}$) with the parameter $\gamma=0.5$.

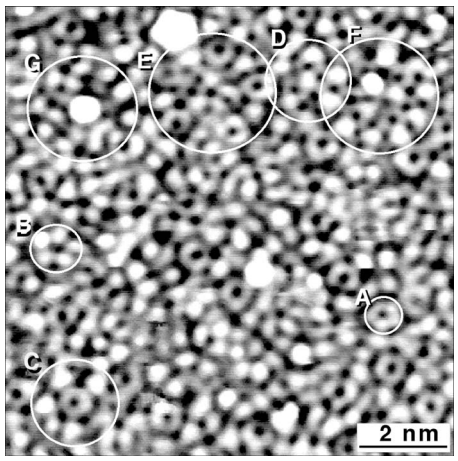

FIG. 9. A high-resolution STM image of the *d*-Al-Co-Ni surface measured by Yuhara *et al.* (Ref. 4). Some of the pentagonal structural elements are marked by circles of various diameters and marked by letters *A*, *B*, *C*, *D*, *E*, *F*, and *G*.

The overall features of the STM images of both surface terminations are quite similar. A brief look on the STM images does not reveal any dramatic differences between both surfaces. The electron density distributions on both surfaces presented in Fig. 6 display much larger differences. However, a closer inspection shows that each surface has its own characteristic structural features. The STM signal is formed predominantly by Al atoms. This is in agreement with the expectation based on the DOS presented in Fig. 4. The STM image of the Al-rich *B* surface is overall a little brighter than that of the TM-rich *A* surface. Nevertheless, both TM atoms Ni and Co also significantly contribute to the STM current. Because of the localized character of *d* states on the TM atoms, the contribution of these atoms to the STM current is generally substantially smaller than the contribution of the *s*,*p* electrons on Al atoms. From a somewhat lower partial DOS of the Ni atoms around the Fermi level in comparison with that of the Co atoms (see Fig. 4), one can expect that in the STM image the Co atoms are seen as brighter spots in comparison with the Ni atoms. A detailed inspection of the central pentagon of TM atoms in the *A* surface confirms that it is indeed the case.

C. Comparison of the experimental STM images

Recently we have performed a detailed comparison of calculated and measured STM images of the fivefold surface of

i-Al-Pd-Mn.[44] For several medium-scale (10–15 Å) characteristic atomic configurations (commonly known as "dark stars" and "white flowers") we were able to obtain quantitative agreement in the calculated and experimental images. Figure 9 presents a high-resolution STM image of the *d*-Al-Co-Ni surface measured by Yuhara *et al.*[4] The experimental image was scanned at the tunneling current $I=0.5$ nA and the voltage $V=-0.5$ V. Height profiles of the STM images display a step height of 2 Å between neighboring terraces, compatible with a simultaneous exposure of both *A* and *B* surfaces.

As the reported composition of the decagonal quasicrystal $Al_{72}Co_{16}Ni_{12}$ is different from the composition of our *W* phase, a comparison of the experimental STM image with the simulated ones (Fig. 8) can be performed only on a qualitative basis. In agreement with our simulated images, no significant differences of the STM images of terraces separated by 2-Å steps have been reported. In the experimental STM image some of the pentagonal structural elements are marked by circles of various diameters and marked by letters *A*, *B*, *C*, *D*, *E*, *F*, and *G*. An agreement with the simulated image can be found only for the smallest structural elements—pentagons of bright spots in the circles *A*, *B*, and *C*. The length of the edge of the pentagon with a dark center in the circle *A* can be estimated as ≈3.0 Å. This size is comparable with the value 2.92 Å corresponding to the size of the pentagon of Al or TM atoms inside the pentagonal tiles on the surface *B*, [see the smaller dotted circle in the right part of Fig. 8(b) and compare with Fig. 1(b)]. The distance between the bright spots forming the pentagon in the circle *B* is ≈4.5 Å. This size is comparable with the edge length of 4.68 Å of the pentagonal tiles superposed on the surface *A* [see the dotted circle in Fig. 8(a)]. The structural model [Fig. 1(a)] shows that TM atoms are located at the vertices of these pentagonal tiles. The configuration of bright spots in the circle *C* in Fig. 9 seems to correspond to the decoration of some of the pentagonal tiles on the surface *B* [see the right-hand part of Figs. 1(b) and 8(b)]. In the circle *C* one can recognize bright spots in the form of two concentric pentagons with opposite orientations. While the size of the smaller one is the same as in the circle *A* the size of the larger one is well compatible with a length of 7.68 Å, the length of the edge of the pentagonal tile on the surface *B*. As the surface area of our *W* approximant is limited, one cannot expect to find the larger pentagonal structural elements marked by circles *E*–*G* in the experimental STM image in Fig. 9. On the other hand, in the experimental STM image we did not find configurations of bright spots characteristic for the *W* phase that we observe in Fig. 8—for instance, the configurations of spots in a form of a pentagon centered by a bright spot [unlabeled circle in right part of Fig. 8(a) or in left part of Fig. 8(b)], although the configuration of the bright spots marked in Fig. 9 by the circle *D* resembles these configurations. We note that these pentagonal configurations belong to the layers of the 20-Å decagonal columnar cluster.

VI. CONCLUSIONS

The structure, stability, and electronic properties of the tenfold surface of a decagonal Al-Co-Ni quasicrystal have been investigated using *ab initio* density-functional methods. Our structural model is based on the approximant *W*-(AlCoNi) phase which is closely related to the decagonal Al-Co-Ni quasicrystal. The bulk quasicrystal can be cleaved at the flat *A* plane or at the puckered *B* plane. We investigate the stability and the electronic properties of the surface for both possible terminations. Our *ab initio* investigations show that the structure of both surfaces is stable against surface reconstruction. Atoms at the surface remain essentially at their bulk position. There is no surface reconstruction; relaxations by interatomic forces have only minimal effect on the atomic positions. We did not observe any significant changes of interlayer spacing of the surface layers in comparison with the interlayer spacing in the bulk.

The electronic structure of the bulk *W*-(AlCoNi) phase is characterized by a pseudogap at the Fermi level. This is a surprising observation and could revive the discussion on the role of the Hume-Rothery mechanism in stabilizing the decagonal quasicrystals. However, we assume that instead of invoking a Hume-Rothery-type Fermi-surface Brillouin-zone interaction the pseudogap reflects the enhanced covalency in the interatomic Al-M bonding of the atoms in the quasicrystal. The pseudogap in the surface local DOS is partially covered and the positions of *d* bands of both transition metals undergo a substantial shift towards lower binding energies. A similar behavior of the surface DOS we observed also in the case of the *i*-Al-Pd-Mn quasicrystal.[5] At the surface of the *W*-(AlCoNi) phase there are no special structural defects such as, e.g., the surface vacancies observed at the fivefold surface of *i*-Al-Pd-Mn. Otherwise the roughness of both *W*-(AlCoNi) surfaces is similar to that of the fivefold *i*-Al-Pd-Mn surface. In terms of variation of the local electron density the roughness of the flat *A* surface is comparable to that of the puckered *B* surface. The simulated STM images of both surfaces show that despite their significantly different atomic structure and chemical composition both planes exhibit quite similar STM images, albeit each of them has its own characteristic details. Present work is devoted to the investigation of quasiperiodic elemental overlayers, using our model of the tenfold surface as a template.

ACKNOWLEDGMENTS

We thank J. Yuhara and M. Schmid for permission to reproduce the atomically resolved STM image (Fig. 9) from their work. This work has been supported by the Austrian Ministry for Education, Science and Art through the Center for Computational Materials Science and by the Austrian Science Funds through the National Research Network "Nanostructures at Surfaces." M.K. is also grateful for support from the Grant Agency for Science of Slovakia (Grant No. 2/5096/25) and from the Agency for Support of Science and Technology (Grant Nos. APVT-51021102, APVT-51052702, and SO-51/03R80603).

[1] R. McGrath, J. Ledieu, E. J. Cox, and R. D. Diehl, J. Phys.: Condens. Matter **14**, R119 (2002).
[2] M. Kishida, Y. Kamimura, R. Tamura, K. Edagawa, S. Takeuchi, T. Sato, Y. Yokoyama, J. Q. Guo, and A. P. Tsai, Phys. Rev. B **65**, 094208 (2002).
[3] N. Ferralis, K. Pussi, E. J. Cox, M. Gierer, J. Ledieu, I. R. Fisher, C. J. Jenks, M. Lindroos, R. McGrath, and R. D. Diehl, Phys. Rev. B **69**, 153404 (2004).
[4] J. Yuhara, J. Klikovits, M. Schmid, P. Varga, Y. Yokoyama, T. Shishido, and K. Soda, Phys. Rev. B **70**, 024203 (2004).
[5] M. Krajčí and J. Hafner, Phys. Rev. B **71**, 054202 (2005).
[6] S. E. Burkov, Phys. Rev. Lett. **67**, 614 (1991).
[7] K. Hiraga, F. J. Lincoln, and W. Sun, Mater. Trans., JIM **32**, 308 (1991).
[8] K. Hiraga, W. Sun, and A. Yamamoto, Mater. Trans., JIM **35**, 657 (1994).
[9] S. Ritsch, C. Beeli, and H. U. Nissen, Philos. Mag. Lett. **74**, 203 (1996).
[10] A. Yamamoto and S. Weber, Phys. Rev. Lett. **78**, 4430 (1997).
[11] M. Krajčí, J. Hafner, and M. Mihalkovič, Phys. Rev. B **62**, 243 (2000).
[12] E. Abe, K. Saitoh, H. Takakura, A. P. Tsai, P. J. Steinhardt, and H. C. Jeong, Phys. Rev. Lett. **84**, 4609 (2000).
[13] Y. Yan and S. J. Pennycook, Phys. Rev. B **61**, 14291 (2000).
[14] A. Cervellino, T. Haibach, and W. Steurer, Acta Crystallogr., Sect. B: Struct. Sci. **58**, 8 (2002).
[15] M. Mihalkovič, I. Al-Lehyani, E. Cockayne, C. L. Henley, N. Moghadam, J. A. Moriarty, Y. Wang, and M. Widom, Phys. Rev. B **65**, 104205 (2002).
[16] K. Sugiyama, S. Nishimura, and K. Hiraga, J. Alloys Compd. **342**, 65 (2002).
[17] M. Kobas, T. Weber, and W. Steurer, Phys. Rev. B **71**, 224205 (2005); **71**, 224206 (2005).
[18] K. Edagawa, H. Tamaru, S. Yamaguchi, K. Suzuki, and S. Takeuchi, Phys. Rev. B **50**, 12413 (1994).
[19] B. Grushko, in *Proceedings of Aperiodic 94*, edited by G. Chapuis and W. Paciorek (World Scientific, Singapore, 1995), p. 573.
[20] A. Fujiwara, A. Inoue, and A. P. Tsai, in *Proceedings of the 6th International Conference on Quasicrystals, Tokyo 1997*, edited by S. Takeuchi and T. Fujiwara (World Scientific, Singapore, 1997), p. 341.
[21] S. Ritsch, C. Beeli, H.-U. Nissen, T. Gödecke, M. Scheffer, and R. Lück, Philos. Mag. Lett. **78**, 67 (1998) and further references therein.
[22] S. Deloudi, M. Kobas, and W. Steurer, in *Proceedings of the 9th International Conference on Quasicrystals*, edited by P. Thiel, C. Jenks, and D. Sordelet, Philos. Mag. **86**, 581 (2006).
[23] G. Kresse and J. Furthmüller, Comput. Mater. Sci. **6**, 15 (1996); **54**, 11169 (1996).
[24] G. Kresse and D. Joubert, Phys. Rev. B **59**, 1758 (1999).
[25] J. P. Perdew and Y. Wang, Phys. Rev. B **45**, 13244 (1992).
[26] M. Mihalkovič and M. Widom, alloy database at http://alloy.phys.cmu.edu/
[27] K. J. Franke, H. R. Sharma, W. Theis, P. Gille, Ph. Ebert, and K. H. Rieder, Phys. Rev. Lett. **89**, 156104 (2002).
[28] C. L. Henley and M. Mihalkovič, in *Proceedings of the 9th International Conference on Quasicrystals*, edited by P. Thiel, C. Jenks, and D. Sordelet, Philos. Mag. (to be published).
[29] A. Groß, *Theoretical Surface Science* (Springer, Berlin, 2003).
[30] M. Krajčí and J. Hafner, Phys. Rev. B **46**, 10669 (1992).
[31] M. Windisch, J. Hafner, M. Krajčí, and M. Mihalkovič, Phys. Rev. B **49**, 8701 (1994).
[32] F. Gähler and S. Hocker, J. Non-Cryst. Solids **334–335**, 308 (2004).
[33] J. Hafner and M. Krajčí, Phys. Rev. Lett. **68**, 2321 (1992).
[34] J. Hafner and M. Krajčí, Phys. Rev. B **47**, 11795 (1993).
[35] U. Mizutani, in *The Science of Complex Alloy Phases*, edited by T. B. Massalski and P. E. A. Turchi (TMS, Warrendale, PA, 2005), p. 1.
[36] G. Trambly de Laissardière, D. Nguyen-Manh, and D. Mayou, Prog. Mater. Sci. **50**, 679 (2005).
[37] M. Krajčí and J. Hafner, J. Phys.: Condens. Matter **13**, 3817 (2000).
[38] M. Krajčí, J. Hafner, and M. Mihalkovič, Europhys. Lett. **34**, 207 (1996).
[39] Z. M. Stadnik, G. W. Zhang, A.-P. Tsai, and A. Inoue, Phys. Rev. B **51**, 11358 (1995).
[40] Z. M. Stadnik, D. Purdie, M. Garnier, Y. Baer, A.-P. Tsai, A. Inoue, K. Edagawa, S. Takeuchi, and K. H. J. Buschow, Phys. Rev. B **55**, 10938 (1997).
[41] Z. M. Stadnik, D. Purdie, M. Garnier, Y. Baer, A.-P. Tsai, A. Inoue, K. Edagawa, and S. Takeuchi, in *Proceedings of the 6th International Conference on Quasicrystals, Tokyo 1997*, edited by S. Takeuchi and T. Fujiwara (World Scientific, Singapore, 1997), p. 563.
[42] E. Belin-Ferré, Z. Dankhazi, V. Fournée, A. Sadoc, C. Berger, H. Müller, and H. Kirchmayr, J. Phys.: Condens. Matter **8**, 6213 (1996).
[43] T. Suzuki, H. R. Sharma, T. Nishimura, M. Shimoda, Y. Yamauchi, and A.-P. Tsai, Phys. Rev. B **72**, 115427 (2005).
[44] M. Krajčí, J. Hafner, J. Ledieu, and R. McGrath, Phys. Rev. B **73**, 024202 (2006).
[45] M. Krajčí and J. Hafner, J. Phys.: Condens. Matter **14**, 1865 (2002).
[46] M. Krajčí and J. Hafner, J. Phys.: Condens. Matter **14**, 5755 (2002).
[47] M. Krajčí and J. Hafner, J. Phys.: Condens. Matter **14**, 7201 (2002).
[48] M. Jahnátek, M. Krajčí, and J. Hafner, J. Phys.: Condens. Matter **15**, 5675 (2003).
[49] J. Tersoff and D. R. Hamann, Phys. Rev. B **31**, 805 (1985).